6-1984

Electrochemical Studies of Antimony(III) and Antimony(V) in Molten Mixtures of Aluminum Chloride and Butylpyridinium Chloride

Dhia A. Habboush
Sacred Heart University, habboushd@sacredheart.edu

Robert A. Osteryoung

Recommended Citation

Habboush, D. A., & Oysteryoung, R. A. (1984). Electrochemical Studies of Antimony(II1) and Antimony (V) in Molten Mixtures of Aluminum Chloride and Butylpyridinium Chloride. Inorganic Chemistry, 23, 1726-1734. doi:10.1021/ic00180a018

Crystal data are given in Table V.

Acknowledgment. The authors are grateful to the National Science Foundation for financial support (Grant CHE 82-06169) and the Wrubel Computing Center, Indiana University, for a generous gift of computing time.

Registry No. **1**, 85923-35-9; **2**, 89656-65-5; **3**, 61916-35-6; **4**, 89708-59-8; **5a**, 85939-38-4; **6a**, 89708-60-1; **7a**, 89708-61-2; $TaCl_4(dmpe)_2$, 61916-34-5; $NbCl_4(dmpe)_2$, 61202-65-1; $TaCl_5$, 7721-01-9; $NbCl_5$, 10026-12-7; D, 7782-39-0.

Supplementary Material Available: Listings of phosphine hydrogen atom positions, anisotropic thermal parameters and observed and calculated structure factors for $TaCl_2H_2(PMe_3)_4$ (**5a**) and $TaCl_2H_2(dmpe)_2$ (**6a**) and experimental ESR spectra of **6a** and **6b** (22 pages). Ordering information is given on any current masthead page. Complete structural reports on **5a** (MSC Report No. 82934) and **6a** (MSC Report No. 83913) are available, in microfiche form only, from the Chemistry Library, Indiana University.

Contribution from the Department of Chemistry, State University of New York at Buffalo, Buffalo, New York 14214

Electrochemical Studies of Antimony(III) and Antimony(V) in Molten Mixtures of Aluminum Chloride and Butylpyridinium Chloride

DHIA A. HABBOUSH† and ROBERT A. OSTERYOUNG*

Received May 24, 1983

Electrochemical studies of Sb, Sb(III), and Sb(V) have been carried out in molten mixtures of $AlCl_3$ and *N*-1-butylpyridinium chloride (BuPyCl) at 40 °C, as a function of melt composition. Analysis of measurements in the acidic melts indicates $SbCl_2^+$ as the dominant species. The reduction of this species on glassy carbon exhibits irreversible behavior. In the basic melts, $SbCl_4^-$ and $SbCl_6^-$ are believed to be the dominant species. The reduction of Sb(III) to Sb on glassy carbon also showed irreversible behavior while its oxidation to Sb(V) revealed a quasi-reversible behavior. No Sb(III) oxidation was observed in the acidic melts.

Introduction

Molten mixtures of $AlCl_3$ and *N*-1-butylpyridinium chloride (BuPyCl) have been shown to be useful and interesting solvents for a variety of electrochemical and spectroscopic studies.[1-7] The mixtures, of composition ranging from 2:1 to 0.75:1 (mol) of $AlCl_3$:BuPyCl, are liquids at essentially ambient temperatures.[2,8] They are ionic liquids, and their composition can be adjusted to change their acid–base properties which, in turn, determine their oxidation–reduction and coordination chemistry. Raman and infrared spectroscopic studies showed that the dominant Al-containing species in the system are $AlCl_4^-$ and $Al_2Cl_7^-$ ions.[8,9] The acid–base equilibrium in these solvents has been studied potentiometrically, by employing Al indicator electrodes, and the equilibrium

$$2AlCl_4^- \rightleftarrows Al_2Cl_7^- + Cl^- \qquad (1)$$

was shown to describe the system across the entire range of compositions mentioned above.[10,11] Electrochemical studies of several organic and inorganic solute species in this and similar systems revealed a pronounced dependence of the solute chemistry and electrochemistry on the system acidity.[2,3,6] In the basic (excess BuPyCl) melt, stable chloro complexes of Ni(II), Fe(II), Fe(III), Cu(I), Cu(II), and Co(II) have been reported.[3,6,12,13]

Studies of molten $SbCl_3$ and its mixtures with alkali-metal chloride and/or $AlCl_3$ have reported the formation of several species of antimony.[14-20] As a result of conductance measurements of $AlCl_3$ in molten $SbCl_3$[14] and of KCl in molten $SbCl_3$,[15,16] the presence of $SbCl_2^+$ and $SbCl_4^-$ in these mixtures has been suggested, and the reaction

$$SbCl_3 + AlCl_3 \rightarrow SbCl_2^+ + AlCl_4^- \qquad (2)$$

was proposed for $AlCl_3$ in $SbCl_3$.[14] Raman studies, however, did not give support for the above suggested species and, instead, indicated some interaction between $SbCl_3$ and $AlCl_3$ in their molten equimolar mixture and the possible formation of some higher chloro complexes of antimony in molten mixtures of $SbCl_3$ and KCl.[17] $SbCl_2^+$, produced from reaction 2, has recently been postulated as the species responsible for the chemical oxidation of perylene in molten $SbCl_3$ containing $AlCl_3$.[18] Lower valent Sb species have been suggested as a result of solubility measurements of Sb in molten $SbCl_3$ containing $AlCl_3$[19,20] and CsCl.[20]

We have studied the electrochemistry of Sb in molten mixtures of $AlCl_3$ and BuPyCl to characterize the major species present. Such information would also be useful in any study of organic solutes in solutions of melts containing $SbCl_3$ where the solvent acidity can be varied.[18,21-24]

† Present address: Department of Chemistry, Sacred Heart University, Bridgeport, CT 06606.

(1) Chum, H. L.; Koch, L. L.; Osteryoung, R. A. *J. Am. Chem. Soc.* **1975**, *97*, 3264.
(2) Robinson, J.; Osteryoung, R. A. *J. Am. Chem. Soc.* **1979**, *101*, 323.
(3) Gale, R. J.; Gilbert, B.; Osteryoung, R. A. *Inorg. Chem.* **1979**, *18*, 2723.
(4) Robinson, J.; Osteryoung, R. A. *J. Am. Chem. Soc.* **1980**, *102*, 4415.
(5) Gale, R. J.; Osteryoung, R. A. *J. Electrochem. Soc.* **1980**, *127*, 2167.
(6) Nanjundiah, C.; Shimizu, K.; Osteryoung, R. A. *J. Electrochem. Soc.* **1982**, *129*, 2474. Nanjundiah, C.; Osteryoung, R. A. *Ibid.* **1983**, *130*, 1312.
(7) Gale, R. J.; Job, R. *Inorg. Chem.* **1981**, *20*, 40, 42.
(8) Gale, J. R.; Gilbert, B.; Osteryoung, R. A. *Inorg. Chem.* **1978**, *17*, 2728.
(9) Gale, R. J.; Osteryoung, R. A. *Inorg. Chem.* **1980**, *19*, 2240.
(10) Gale, R. J.; Osteryoung, R. A. *Inorg. Chem.* **1979**, *18*, 1603.
(11) Schoebrechts, J.; Gilbert, B. *J. Electrochem. Soc.* **1981**, *128*, 2679.
(12) Hussey, C. L.; Laher, T. M. *Inorg. Chem.* **1981**, *20*, 4201.
(13) Laher, T. M.; Hussey, C. L. *Inorg. Chem.* **1982**, *21*, 4079.
(14) Texier, P. *Bull. Soc. Chim. Fr.* **1968**, 4716.
(15) Porter, G. B.; Baughan, E. C. *J. Chem. Soc.* **1958**, 744.
(16) Davis, A. G.; Baughan, E. C. *J. Chem. Soc.* **1961**, 1711.
(17) Fung, K. W.; Begun, G. M.; Mamantov, G. *Inorg. Chem.* **1973**, *12*, 53.
(18) Sorlie, M.; Smith, G. P.; Norvell, V. E.; Mamantov, G.; Klatt, L. N. *J. Electrochem. Soc.* **1981**, *128*, 333.
(19) Corbett, J. D. "Progress in Inorganic Chemistry"; Lippard, S. J., Ed.; Wiley: New York, 1976; Vol. 21, pp 129–158.
(20) Sorlie, M.; Smith, G. P. *J. Inorg. Nucl. Chem.* **1981**, *43*, 931.
(21) Buchanan, A. C., III; Dworkin, A. S.; Smith, G. P. *J. Am. Chem. Soc.* **1980**, *102*, 5262.

0020-1669/84/1323-1726$01.50/0

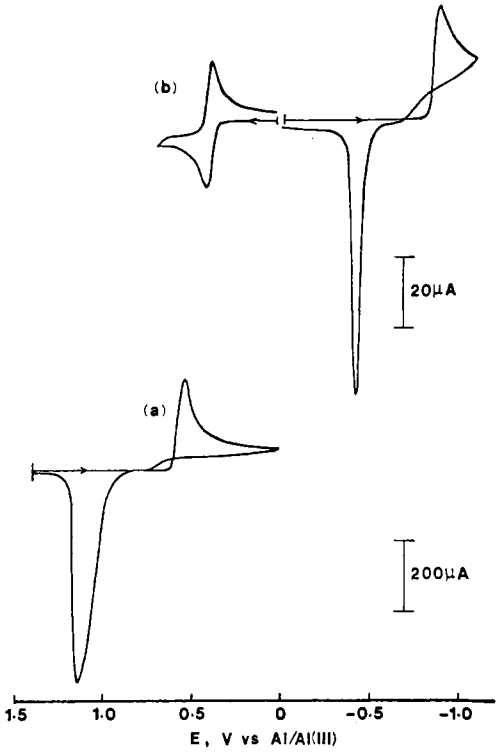

Figure 1. Cyclic voltammograms of Sb(III) melt solutions: a, 7.0 × 10^{-3} M in 1.5:1 melt, v = 20 mV s^{-1}; b, 6.3 × 10^{-3} M in 0.8:1 melt, v = 5 mV s^{-1}.

Experimental Section

Preparation of $AlCl_3$ and *n*-butylpyridinium chloride has been described elsewhere.[2] Sb(III) was generated in situ by anodic dissolution of an antimony rod (Alfa Products) by constant-potential coulometry or by the addition of anhydrous $SbCl_3$ (Alfa Products). The antimony rod was cleaned in concentrated HCl, washed with water and acetone, and dried. Aluminum wire (Alfa Products) was cleaned in a 30:30:40 volume mixture of concentrated sulfuric, nitric, and phosphoric acids, washed with water and acetone, and dried.

A homemade glass container was employed as the electrolytic cell and was covered with a Teflon lid with holes for reference electrode and counterelectrode compartments, a thermocouple well, an antimony rod, and the rotating disk electrode. The cell assembly was placed in a furnace whose temperature was controlled at 40 ± 1 °C by a Thermo Electric temperature controller. A rotating glassy-carbon disk electrode (RGCDE), with an area of 0.196 cm^2, was employed; its surface was polished with 0.2-μm alumina on a wet polishing cloth and washed in water. The reference electrode and counterelectrode were Al wires dipped in 2:1 $AlCl_3$:BuPyCl melt, and both were separated from the rotating disk electrode compartment by fine glass frits (porosity E).

An EG&G PARC 175 programmer and PARC 173 potentiostat with a Model 179 coulometer were used for all voltammetric and coulometric experiments, which were recorded on an HP 7046 X-Y recorder. Potentiometric measurements were made with a Keithly 168 digital voltmeter with a voltage follower in the circuit. A Pine Instrument Co. ASR rotator was employed for all rotating electrode experiments, which were carried out in a Vacuum Atmospheres drybox with a circulating, purified argon atmosphere.

Melts were prepared by mixing weighed amounts of purified $AlCl_3$ and BuPyCl.[2,10] The electrode surface was conditioned by holding at an initial potential, where no reaction of primary interest took place, until the background current had decayed to a low, constant value. Constant-potential coulometric experiments were performed by changing the potential from a value where no current passed to one where the desired reaction would take place. The solutions were stirred during the coulometric experiments.

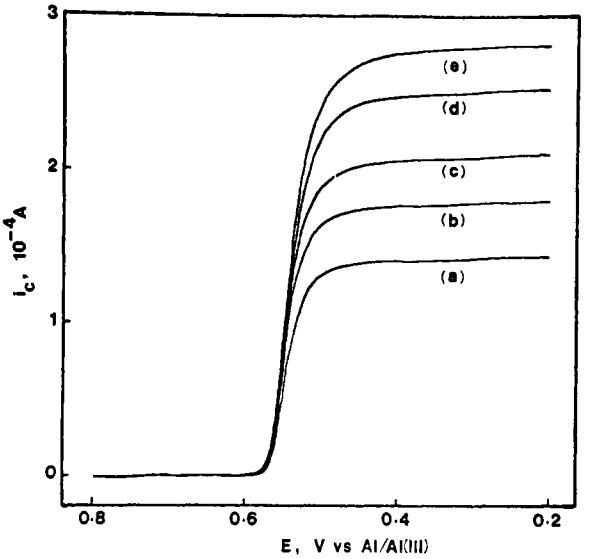

Figure 2. Voltammograms of a 6.2 × 10^{-3} M solution of Sb(III) in 1.24:1 melt, at RGCDE. Rotation rate/rpm: a, 450; b, 650; c, 960; d, 1270; e, 1670.

Results and Discussion

$SbCl_3$ dissolved readily in molten mixtures of $AlCl_3$ and BuPyCl (both acidic and basic) to form almost colorless solutions. Representative cyclic voltammograms of these solutions, at a glassy-carbon electrode vs. an Al/Al(III) reference, are shown in Figure 1 and yield one cathodic wave for solutions in acidic melts and two waves, one cathodic and one anodic, for solutions in basic melts. Solutions obtained from anodic dissolution of antimony metal at constant potentials in these melts (at +1.3 V in the acidic 2:1 and at −0.2 V in the basic 0.75:1 $AlCl_3$:BuPyCl melt) gave cyclic voltammograms similar to those of the $SbCl_3$ solutions.

Acidic Melts. Table I lists data obtained from cyclic voltammetry of solutions of $SbCl_3$ in acidic melts. The cathodic current peak for Sb deposition shifts negatively with increasing scan rate, which is indicative of either slow charge-transfer reaction rate (irreversible behavior) or, more likely, nucleation overvoltage. A negative shift of this peak with decreasing acidity is also evident and would be expected if the complexing ligand is either one of two species present in these melts, namely Cl^- or $AlCl_4^-$, rather than $Al_2Cl_7^-$. The reverse scan produced one stripping peak; the charge under the anodic stripping peak equaled that on the cathodic scan.

Voltammograms of these solutions were also obtained on the RGCDE and are shown in Figure 2. Plots of the limiting cathodic currents at potentials on the plateau (i_{lc}), for solutions in various acidic melts, vs. the square root of the rotation rate ($\omega^{1/2}$) were linear (Figure 3) and passed through the origin, indicating that the reaction is convective diffusion controlled in the limiting region.

To confirm the oxidation state of the antimony species present in these solutions, constant-potential coulometry for the deposition of antimony (from 7.7 mL of a 11.1 × 10^{-3} M $SbCl_3$ solution in a 2:1 melt) was carried out at +0.4 V on a glassy-carbon electrode of a large area; the +0.4 V value corresponds to a potential on the diffusion limiting plateau of the reduction wave (Figure 2). This electrolysis was stopped at various times, and voltammograms were run at a RGCDE. A plot of the cathodic charge (Q_c) vs. i_{lc} was linear, and thus Q_c for a complete reduction to Sb was obtained by extrapolation to the Q_c axis. The results of this experiment established that the oxidation state of antimony in solution was +3; Q_c found was 25 C compared with that calculated for a complete

(22) Buchanan, A. C., III; Dworkin, A. S.; Smith, G. P. *J. Org. Chem.* **1981**, *46*, 471.
(23) Buchanan, A. C., III; Livingston, R.; Dworkin, A. S.; Smith, G. P. *J. Phys. Chem.* **1980**, *84*, 423.
(24) Buchanan, A. C., III; Dworkin, A. S.; Brynestad, J.; Gilpatrick, L. O.; Poutsma, M. L.; Smith, G. P. *J. Am. Chem. Soc.* **1979**, *101*, 5430.

Table I. Dependence of E_{p_c}, E_{p_a}, $E^{\circ\prime}$, and $E^{\circ\prime}{}_2$ for Sb(III)/Sb on Melt Composition

N_A/N_B	v, mV s^{-1}	E_{p_c}, V	E_{p_a}, V	$E^{\circ\prime}$,[a,c] V	$E^{\circ\prime}{}_2$,[b,c] V	$E^{\circ\prime}$,[a,d] V	$E^{\circ\prime}{}_2$,[b,d] V
2.00	10	0.665	1.145	1.007	0.380	0.988	0.359
	20	0.640	1.165				
	50	0.580	1.210				
	100	0.550	1.265				
	200	0.515	1.325				
	500	0.455	1.390				
1.95				0.977	0.399		
1.92				0.963	0.402		
1.83				0.938	0.403		
1.64				0.901	0.397		
1.50	20	0.530	1.110			0.833	0.346
1.44				0.877	0.396		
1.24	20	0.495	1.080	0.848	0.390		
1.09	20	0.435	1.045			0.755	0.323
1.06				0.811	0.387		
1.04				0.773	0.362		
1.02				0.758	0.368		
1.01	20	0.400	1.015	0.736	0.392	0.708	0.331
					av 0.389 ± 0.014		
0.98				−0.431	−0.521		
0.94				−0.471	−0.521		
0.91	5	−0.775	−0.345				
	10	−0.820	−0.320				
	20	−0.865	−0.305				
	50	−0.925	−0.280				
0.87				−0.504	−0.525		
0.81				−0.516	−0.523		
0.80	5	−0.885	−0.420				
0.75	5	−0.910	−0.430	−0.527	−0.523		
					av −0.523 ± 0.002		

[a] $E^{\circ\prime} = E_{eq} - (RT/3F) \ln [Sb(III)]$. [b] $E^{\circ\prime}{}_2 = E_{eq} - (RT/3F) \ln [Sb(III)] + (pRT/3F) \ln [Cl^-]$; $p = 2$ for $N_A/N_B > 1$, $p = 4$ for $N_A/N_B < 1$. [c] From potentiometry. [d] From voltammograms of Sb(III) solutions on RGCDE obtained from a reverse scan.

Table II. Dependence of $D_{Sb(III)}$ and $\eta D_{Sb(III)}$ on the Melt Composition in the Acidic Region

N_A/N_B	η,[a] g cm^{-1} s^{-1}	$D_{Sb(III)}$, 10^{-7} cm^2 s^{-1}	$\eta D_{Sb(III)}$, 10^{-7} g cm s^{-2}
2.00	0.145	8.15	1.18
1.50	0.175	6.88	1.20
1.24	0.195	6.02	1.17
1.09	0.205	5.76	1.18
1.01	0.215	5.58	1.20
			av 1.19 ± 0.01

[a] Reference 6.

reduction of Sb(III) to Sb, 24.3 C.

The values of the limiting currents, obtained from the voltammograms at the RGCDE (Figure 2), were used to calculate the diffusion coefficients (D), of the Sb(III) species in various acidic melts, from the Levich equation

$$i_l = 0.620nFAD^{2/3}\omega^{1/2}\nu^{-1/3}C^* \quad (3)$$

where ν is the kinematic viscosity (viscosity divided by density), C^* is the concentration of the electroactive species in the bulk in units of mol cm^{-3}, and the other symbols have their usual meanings. The results of these calculations, along with the products of ηD, are tabulated in Table II. The ηD product was found to be constant across the entire range of acidity investigated for the Sb(III) species in acidic melts. Thus, the Stokes–Einstein relation

$$D = kT/6\eta\pi r \quad (4)$$

where k is the Boltzmann constant and r is the radius of the diffusing species, was obeyed.

Initial attempts to measure a stable value for the potential of the Sb(III)/Sb couple were unsuccessful. This variation in potential was attributed to a slight oxidation of the antimony metal into the melt. This oxidation was evident when cyclic voltammetry of a 2:1 melt, following immersion of an antimony rod into it for 1 h, gave rise to a voltammogram similar to that of curve a in Figure 1. The concentration of Sb(III) after this period was estimated as 0.1×10^{-3} M. An additional 24-h immersion increased the concentration of the Sb(III) by about 30%. The possibility that this formation of Sb(III) resulted from dissolution of an oxide film on the Sb metal was ruled out when it was found that an antimony rod, previously held in a similar melt for several weeks, gave rise to a similar solubility of Sb(III) after 18 h of immersion in a new melt. These observations are analogous to an apparent spontaneous oxidation of ferrocene by the acidic melt.[25] Recent work on the reduction of "water" in the melt indicates that the reduction of "proton" takes place at potentials close to, but slightly positive of, the Sb–Sb(III) potential in either acidic or basic melts.[26] This suggests that Sb might have been oxidized by a proton-containing species, possibly an –Al–O–H entity,[27] to yield Sb(III). Part of the reason may also have been a result of leakage of the melt from the bulk solution to the reference compartment, thus changing melt composition in that compartment, and hence the reference potential.

While potentiometric measurements were ultimately obtained (see below), the following procedure was employed to obtain estimates of the Sb–Sb(III) potential under the conditions referred to above. Voltammograms of Sb(III) solutions on a RGCDE (Figure 4) obtained on a reverse scan, i.e., following oxidation of the deposited Sb metal from the electrode surface, gave a constant value for the zero crossing potential as a function of electrode rotation rate. This zero-current crossing potential, as a function of melt composition, was utilized as the equilibrium potential of the Sb(III)/Sb couple to obtain an indication of the nature and number of ligands bound to Sb(III). Values of $E^{\circ\prime}$ so obtained are shown in Table I for comparison with those obtained from direct

(25) Karpinski, Z.; Nanjundiah, C.; Osteryoung, R. A., to be submitted for publication.
(26) Sahami, S.; Osteryoung, R. A. *Anal. Chem.* **1983**, *55*, 1970.
(27) Tait, S.; Osteryoung, R. A., to be submitted for publication.

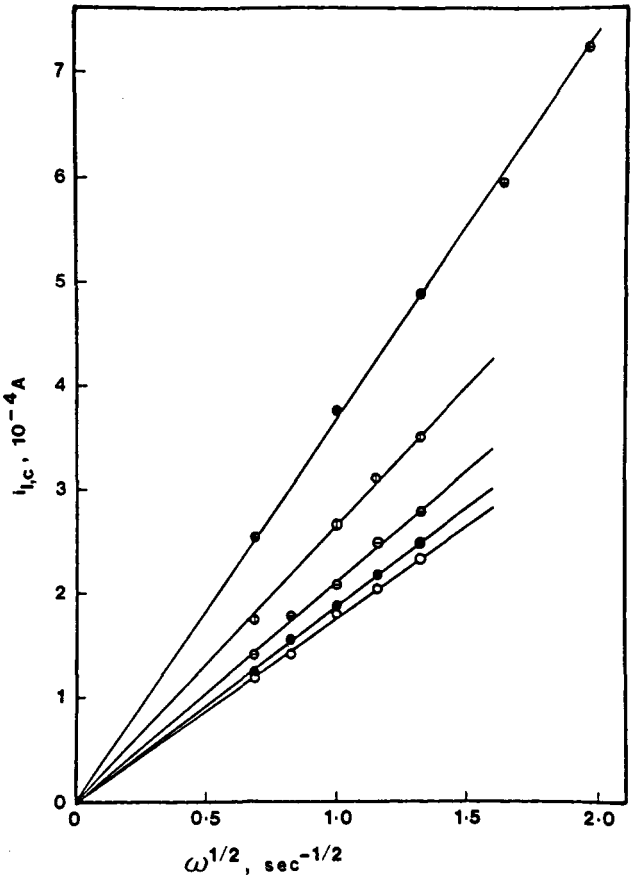

Figure 3. Limiting cathodic currents for the reduction of Sb(III) vs. $\omega^{1/2}$: ⊗, 8.2×10^{-3} M in 2:1 melt; ○, 7.0×10^{-3} M in 1.5:1 melt; ⊖, 6.2×10^{-3} M in 1.24:1 melt; ●, 5.7×10^{-3} M in 1.09:1 melt; ○, 5.5×10^{-3} M in 1.01:1 melt.

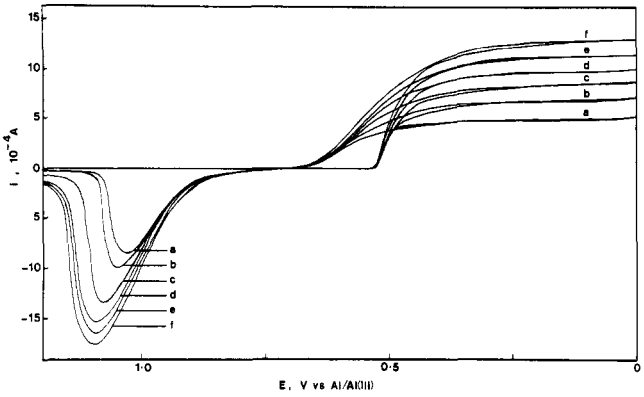

Figure 4. Voltammograms of a 19.5×10^{-3} M solution of Sb(III) in 1.09:1 melt, at RGCDE. Rotation rate/rpm: a, 600; b, 1200; c, 1800; d, 2400; e, 3000; f, 3600.

potentiometry, and a plot of this Sb(III)/Sb potential vs. ln [Cl^-] is shown as curve b in Figure 5. The slope of this line is 19.8 mV, not far from the theoretical slope for $p = 2$; $2RT/3F = 18$ mV at 40 °C (see below).

Under conditions where, finally, a stable Sb(III)/Sb potential could be obtained from direct potentiometry, the potential of the Sb(III)/Sb couple was measured by conventional means and as a function of the melt composition. The potential of the couple—and the following discussion refers to both the direct potentiometry and the "zero-current crossing potential" measurement referred to above—depends on the binding ligand concentration according to the relation

$$E_{eq} = E^\circ{}_1 + (RT/nF) \ln (C_t/C^\ominus) - (RT/nF) \ln (1 + \beta_1[L^-] + \beta_2[L^-]^2 + ...) \quad (5)$$

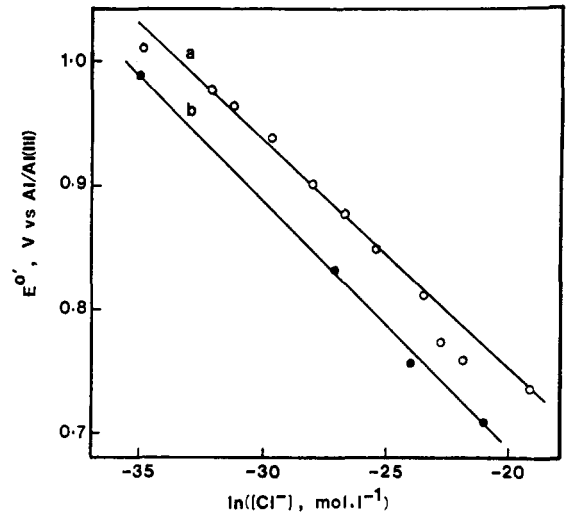

Figure 5. Plots of $E^{\circ\prime}$ vs. ln [Cl^-] for the Sb(III)/Sb couple in acidic melts: a, from potentiometry; b, from voltammograms of Sb(III) solutions on RGCDE obtained from a reverse scan (see text).

where E_{eq} is the Sb(III)/Sb equilibrium potential, $E^\circ{}_1$ is the formal potential of the couple in the absence of free ligand (i.e., no complex formation), C_t is the total concentration of all Sb(III) species, [L^-] is the concentration of the free ligand, $C^\ominus$ is the standard concentration defined as 1 mol L^{-1}, and the β's are the overall stability constants for the various complex species. Equation 5 may be used to determine the number of ligands and to evaluate the stability constants. In order to do so we introduced a new formal potential $E^{\circ\prime}$ defined as

$$E^{\circ\prime} = E^\circ{}_1 - (RT/nF) \ln (1 + \beta_1[L^-] + \beta_2[L^-]^2 + ...) \quad (6)$$

which is independent of species concentration and can be calculated from the relation

$$E_{eq} = E^{\circ\prime} + (RT/nF) \ln (C_t/C^\ominus) \quad (7)$$

which is a reduced form of eq 5. A plot of $E^{\circ\prime}$ vs. ln [Cl^-] (Figure 5, curve a) gave a straight line over the melt composition range 2:1 to 1.01:1, indicating one dominant complex. Hence, the polynomial equation (6) can be reduced to the simple relation

$$E^{\circ\prime} = E^\circ{}_1 - (RT/nF) \ln \beta_p - (pRT/nF) \ln ([L^-]/C^\ominus) \quad (8)$$

where p is the number of ligands.

The slope of the curve a in Figure 5 permits evaluation of the number of the ligands, p. The experimental slope is 18.4 mV, yielding a value of $p = 2$; $2RT/3F = 18$ mV at 40 °C. The chloride concentrations in these acidic melts were calculated from equilibrium 1 and a value of the equilibrium constant of 9.5×10^{-13};[3] corrections for one chloride, furnished by $SbCl_3$, were made in these calculations. Thus, these plots of the potential of the Sb(III)/Sb potential in Figure 5 appear to indicate that $SbCl_2^+$ is the predominant Sb(III) species existing in the acidic melt.

Provided that a value of $E^\circ{}_1$ is known, a value of $\beta_{SbCl_2^+}$ may be calculated. In the case of calculating such stability constants in chloroaluminate melts, a value of E_1° is usually taken at a fixed melt composition. Table I presents values for $E^{\circ\prime}$, defined as per eq 7. We *arbitrarily* choose $E^{\circ\prime}$ for the 1.1:1 melt (which can be interpolated from the data presented to be 0.83 V), set it equal to $E^\circ{}_1$, and extrapolate the data of curve 1, Figure 5, to ln [Cl^-] = 0, to give a value of what is termed $E^{\circ\prime}{}_2$ in Table I of 0.38 V (which is effectively the first two terms of the right-hand side of eq 8). We can then obtain a value of $\beta_{SbCl_2^+} = 4.0 \times 10^{21}$. *While the calculation of this*

number is straightforward, its meaning is not. In the first place, as pointed out above, choice of a different melt composition to fix $E°_1$ is totally arbitrary; it may, for instance, be taken in a 0.8:1 melt. In the past, $E°_1$ values have been taken in the acidic melts during attempts to obtain formation constants for chloro complexes in the basic melts.[3,6,12,13] Since such $E°_1$ values depend on the mole ratio of aluminum chloride to organic chloride, values of formation constants are also dependent on the choice of $E°_1$ values. Far more important, however, is the fact that a calculation involving a $[Cl^-]$ value based on application of the solvent equilibrium constant, such as carried out here, depends on the specific value of that constant (taken here as 9.5×10^{-13}) to construct a plot such as in Figure 5; the values for ln $[Cl^-]$ are found from the mole ratio of melt employed and the equilibrium constant. A somewhat different value of the solvent constant will simply shift the ln $[Cl^-]$ scale along the axis. It will not change the slope—hence the value for the number of ligands involved in the coordination with Sb(III) in the acid melt—but will drastically alter the value of the derived $\beta_{SbCl_2^+}$. This problem is far less serious in determining chloro-complex constants in a basic melt, since in such a case the concentration of Cl^- is derived from stoichiometric considerations. We point this out because we have recently obtained evidence pointing to the fact that reported equilibrium constants for the BuPyCl–$AlCl_3$ system[10] and/or the related imidazolium chloride–aluminum chloride systems[28] may be significantly in error.[29] While we recognized the problems inherent in such measurements in our earlier work,[10] in which we indicated that our measured values for the equilibrium constant for eq 1 in the BuPyCl–$AlCl_3$ melt were an upper limit, the extent of the error and its consequences do not appear to have been realized.

The formation of $SbCl_2^+$ in these acidic melts, as indicated from the above results, is in agreement with its formation in $SbCl_3$ melts containing $AlCl_3$.[14,16,18] The validity of the Stokes–Einstein relation, as was established earlier, gives support for the formation of one Sb(III) species across the entire acidic region and gives a value of 1.93 Å for the radius of $SbCl_2^+$ species. This radius would appear to be rather small; data would indicate an ionic radius of 3–5 Å might be expected, depending on the geometry of the $SbCl_2^+$ species in solution.[30] Similar calculations based on the finding of the constancy of the ηD product likewise appear to yield values for r which are too small.[6] A modification, appearing to be a better approximation when it is considered that the radius of a moving particle may be similar to that of the media of viscosity η in which it moves, suggests that the 6 in the Stokes–Einstein equation be replaced by a 4. Under those conditions, the values calculated for r are increased by 50%.[31] Since the constancy of the ηD product in these melts appears well verified experimentally, it is not unreasonable to suggest that the use of the modified Stokes–Einstein equation, as proposed by McLaughlin,[31] gives a better indication of the ionic radii of the diffusing species. No consideration is given to solvation, since our measurements give no information regarding that possibility.

Basic Melts. Table I also lists data obtained from the cathodic wave in cyclic voltammograms (Figure 1, curve b) of solutions of $SbCl_3$ in basic melts. A negative shift in the cathodic current peak with increasing scan rate is similar to that observed in acidic melts and indicates either a slow charge-transfer reaction (irreversible behavior) or a nucleation overvoltage. The hysteresis shown on the reverse scan is typical of that noted for nucleation overvoltage deposition processes. A negative shift in the peak potential with decreasing basicity (increasing pCl) of these solutions may be taken as an indication of a chloride coordination. The charge under the anodic stripping peak was equal to that under the cathodic reduction peak. Voltammograms of the cathodic wave at the RGCDE showed no limiting region due to the proximity of the Sb reduction to the negative limit of the melt (at −1.1 V on glassy carbon).

Voltammograms on the RGCDE of a solution of $SbCl_3$ in the 0.75:1 melt, obtained by scanning anodically, are shown in Figure 6. As shown in Figure 7, curve a, a plot of the limiting anodic currents (i_{la}) at potentials on the plateau, vs. $\omega^{1/2}$ was linear and passed through the origin, indicating that the reaction is convective diffusion controlled at the limiting plateau. Similar plots of the currents at potentials on the ascending portion of the wave, however, were not linear, in-

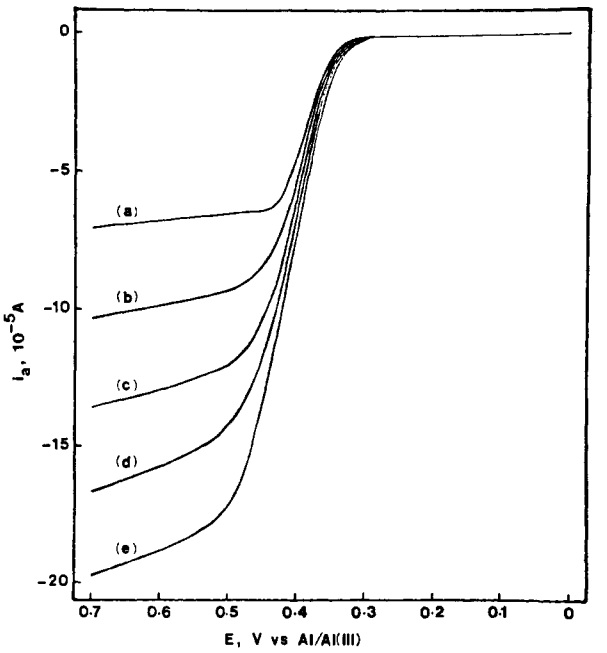

Figure 6. Voltammograms of a 20.4×10^{-3} M solution of Sb(III) in 0.75:1 melt, at RGCDE. Rotation rate/rpm: a, 400; b, 900; c, 1600;, d, 2500; e, 3600.

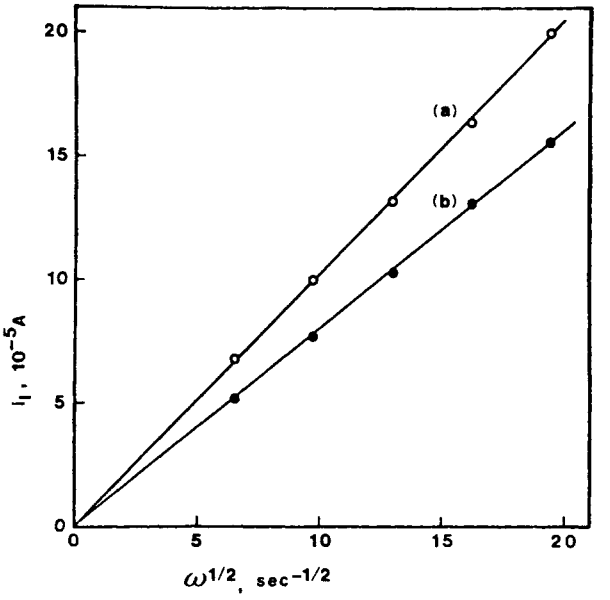

Figure 7. Limiting current vs. $\omega^{1/2}$ in 0.75:1 melt: a, 20.4×10^{-3} M Sb(III); b, 10.2×10^{-3} M Sb(V).

(28) Wilkes, J. S.; Levisky, J. A.; Wilson, R.; Hussey, C. L. *Inorg. Chem.* **1982**, *21*, 1263.
(29) Karpinski, Z.; Osteryoung, R. A. *Inorg. Chem.*, in press.
(30) "Handbook of Chemistry and Physics", 60th ed.; CRC Press: Boca Raton, FL, 1980; p F214.
(31) McLaughlin, E. *Trans. Faraday Soc.* **1959**, *55*, 28.

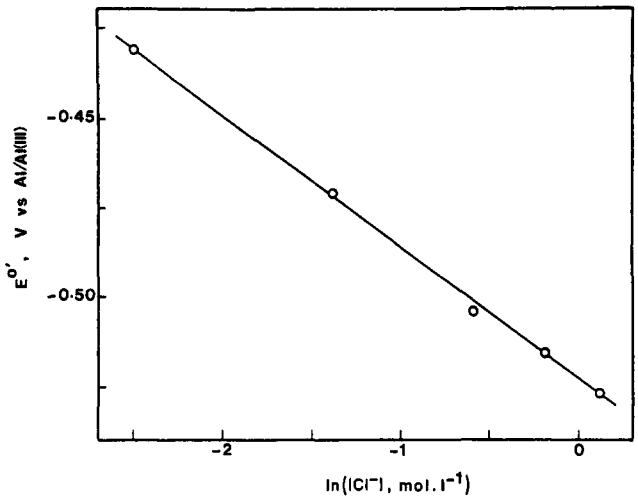

Figure 8. Potentiometric data for the Sb(III)/Sb couple in basic melts as a function of ln [Cl^-].

dicating some kinetic complications.

The oxidation state of the species present in solutions of $SbCl_3$ in the basic melts was established by coulometry in a manner similar to that described for the acidic melts; coulometric deposition of Sb was carried out at −0.9 V, and at several stages the limiting anodic currents at the plateau of the anodic wave (Figure 6) were measured. The results of this experiment indicated the presence of Sb(III) in solution; Q_c found by extrapolation for complete deposition was 15.4 C compared with that calculated for a complete reduction of Sb(III), 15.3 C. Potentiometry of the Sb(III)/Sb couple, in different melt compositions, was performed to study the nature of the complex Sb(III) species present in solution. A plot of $E^{\circ\prime}$, calculated from the potentiometric data as previously described for the acidic melts, vs. ln [Cl^-] was linear (Figure 8). The experimental slope of the plot in Figure 8 at 36.7 mV, yielding a value for the number of ligands of $p = 4$; $4RT/3F = 36$ mV at 40 °C. The chloride concentration in these basic melts was calculated from the amount of BuPyCl in excess of the 1:1 molar ratio of $AlCl_3$:BuPyCl.

Provided that a value of E°_1 is known, a value of β_p may be calculated from eq 8. As discussed above, a value of E°_1 is usually taken at a defined melt composition; again, it must be realized that any melt composition could be employed to determine a value for E°_1, which would result in different values for the stability constant. The 1.1:1 melt has usually been chosen,[6] assuming that the chloride concentration in this melt is negligible (i.e., no complex formation). This method can be used to estimate a stability constant of the $SbCl_4^-$ species although in the acidic melts Sb(III) was shown to exist as $SbCl_2^+$. Taking $E^{\circ\prime}$ in the 1.1:1 melt as 0.83 V and setting it equal to E°_1 as before, and the value for $E^{\circ\prime}$ of −0.52 V, obtained from Figure 8 by extrapolation to ln [Cl^-] = 0, we obtained a value of $\beta_{SbCl_4^-} = 1 \times 10^{65}$.

The ratio of the stability constants of $SbCl_4^-$ to $SbCl_2^+$ can also be calculated. In Table I a formal potential, $E^{\circ\prime}_2$, is defined and its values for different melt compositions are tabulated. As expected from its definition, these values are constant, within tolerable limits, throughout the acidic region and the basic region. This potential, however, can be related to E°_1 by the relation

$$E^{\circ\prime}_2 = E^\circ_1 - (RT/nF) \ln \beta_p \quad (9)$$

Therefore, it is dependent on the stability constant of the Sb(III) species present in solution. Thus, the *difference* between its values in the basic melts and in the acidic melts can be directly related to the relative stability of $SbCl_4^-$ and $SbCl_2^+$. From the average values obtained for $E^{\circ\prime}_2$ in both

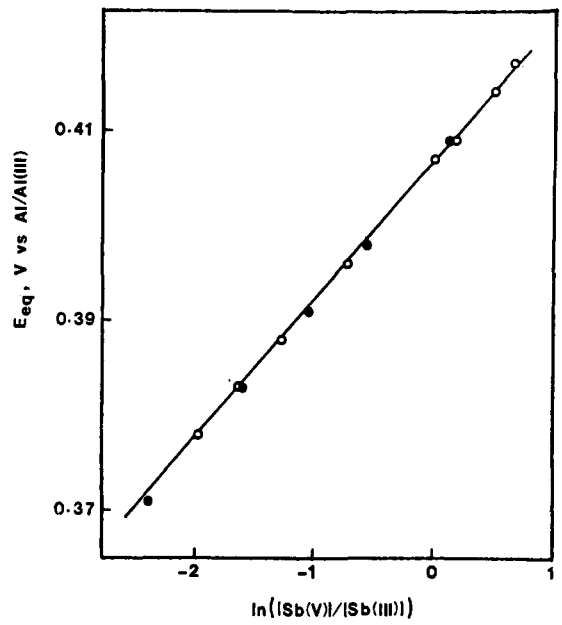

Figure 9. Potentiometric data for the Sb(V)/Sb(III) couple in the 0.75:1 melt.

acidic and basic melts, the ratio of the stability constants of $SbCl_4^-$ to $SbCl_2^+$ was calculated to be 1×10^{44} mol^{-2} L^2. This ratio is independent of any arbitrary choice of E°_1 (provided that they are the same for both acidic and basic melts) since the latter cancels out during its calculation. It is, however, dependent on the value for the solvent dissociation constant.

To establish the oxidation state of the product of the anodic oxidation of the Sb(III) solutions, constant-potential coulometry for the oxidation was carried out at +0.5 V (see Figure 6). The results of this experiment showed that the oxidation state of the product is +5. Q_a found for complete oxidation was 82.5 C compared to that calculated for complete oxidation of Sb(III) to Sb(V) of 81.9 C. The results of potentiometric measurements of the Sb(V)/Sb(III) couple on an inert electrode (glassy carbon) during coulometry gave a linear plot (Figure 9) of the potential vs. the natural logarithm of the ratio of concentrations of Sb(V) to Sb(III) species, as expected from the relation

$$E_{eq} = E^{\circ\prime} + (RT/2F) \ln ([Sb(V)]/[Sb(III)]) \quad (10)$$

where $E^{\circ\prime}$ is the standard formal potential for Sb(V)/Sb(III) species. The slope of the line in Figure 9 was 14.5 mV ($RT/2F$ is 13.5 mV).

Potentiometry of the Sb(V)/Sb(III) system as a function of the melt composition was performed to obtain an indication of the difference between the number of chloride ligands bound to Sb(V) and Sb(III). As shown in Figure 10, a plot of $E^{\circ\prime}$, obtained from eq 10, vs. ln [Cl^-] was linear over the melt composition range 0.75:1 to 0.97:1, indicating one dominant complex for each of the Sb(III) and Sb(V) species. Thus a polynomial equation, similar to eq 6, for Sb(V)/Sb(III) can be reduced to the simple equation

$$E^{\circ\prime} = E^\circ_1 - (RT/2F) \ln (\beta_{p_2}/\beta_{p_1}) - ((p_2 - p_1)RT/2F) \ln [Cl^-]/C^\ominus \quad (11)$$

where E°_1 is the formal standard potential of Sb(V)/Sb(III) in the absence of free chloride (i.e., no complex formation), β_{p_1} and β_{p_2} are the stability constants for Sb(III) and Sb(V) complexes, and p_1 and p_2 are the number of ligands bound to Sb(III) and Sb(V).

The experimental slope of the plot in Figure 10 is 26 mV, yielding a value of $(p_2 - p_1) = 2$; $2RT/2F = 27$ mV. Further calculation to obtain the ratio of β_{p_2}/β_{p_1}, relative to a 1.1:1

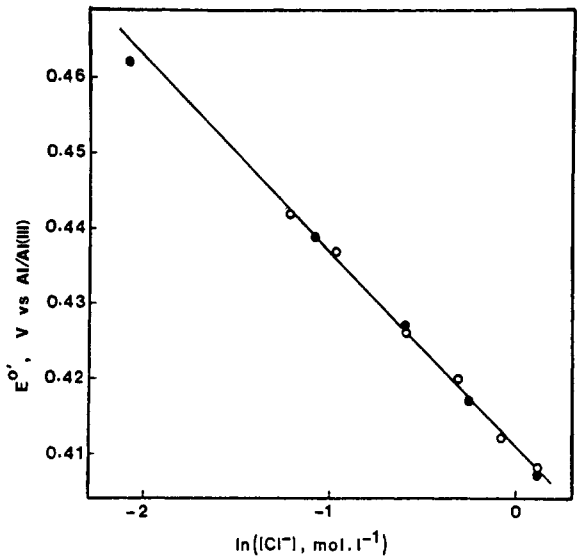

Figure 10. Potentiometric data for Sb(V)/Sb(III) as a function of ln $[Cl^-]$.

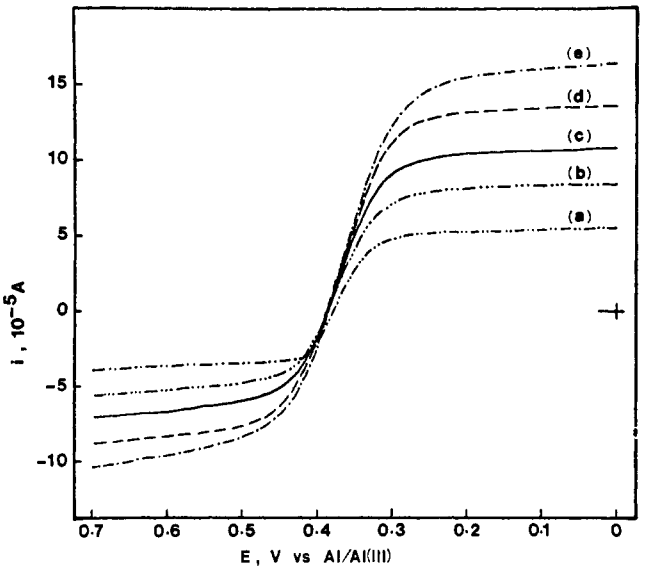

Figure 11. Voltammograms of a solution of Sb(III) and Sb(V) in 0.75:1 melt, at RGCDE ($[Sb(III)] = 10.2 \times 10^{-3}$ M; $[Sb(V)] = 10.2 \times 10^{-3}$ M). Rotation rate/rpm: a, 400; b, 900; c, 1600; d, 2500; e, 3600.

melt or any acidic melt of fixed composition, was not attempted. A ratio calculated in this way will not be useful, since it is relative to the ratio of stability constants of Sb(V) and Sb(III) complexes in the acidic melts, that is an unknown Sb(V) complex species and $SbCl_2^+$.

Although several chloro-complex species of Sb(III) have been reported in the literature, i.e., $SbCl_5^{2-}$,[32] and $SbCl_4^-$,[15,16,33] only the last species has been specifically suggested in solutions of KCl in molten $SbCl_3$;[15,16] possible formation of some uncharacterized higher chloro complexes of Sb(III) in molten mixtures of KCl and $SbCl_3$ has been suggested.[17] On the other hand, the only chloro complex of Sb(V) reported is $SbCl_6^-$.[34] From this and the results above, the formation of $SbCl_4^-$ and $SbCl_6^-$ in the basic melt seems reasonable.

Figure 11 shows voltammograms, obtained on the RGCDE, for a solution of Sb(III) and Sb(V) in a 0.75:1 melt. A plot

(32) Szymanski, H. A.; Yelin, R.; Marabella, L. *J. Chem. Phys.* **1967**, *47*, 1877.
(33) Ahlijah, G. Y.; Goldstein, M. *J. Chem. Soc. A* **1970**, 326.
(34) Burgard, M.; MacCordick, J. *Inorg. Nucl. Chem. Lett.* **1970**, *6*, 599.

Table III. Dependence of $D_{Sb(III)}$, $D_{Sb(V)}$, $\eta D_{Sb(III)}$, and $\eta D_{Sb(V)}$ on the Melt Composition in the Basic Region

N_A/N_B	η,[a] g cm^{-1} s^{-1}	$D_{Sb(III)}$, 10^{-7} cm^2 s^{-1}	$\eta D_{Sb(III)}$, 10^{-8} g cm s^{-2}	$D_{Sb(V)}$, 10^{-7} cm^2 s^{-1}	$\eta D_{Sb(V)}$, 10^{-8} g cm s^{-2}
0.75	0.514	0.79	4.06	1.57	8.07
0.79	0.425	0.93	3.95	1.90	8.08
0.82	0.370	1.08	4.00	2.17	8.03
0.83	0.355	1.12	3.98	2.27	8.06
0.87	0.310	1.32	4.09	2.58	8.00
0.91	0.275	1.50	4.13	2.97	8.17
0.92	0.270	1.53	4.13	2.95	7.96
0.93	0.260	1.59	4.13	3.15	8.19
0.97	0.240	1.69	4.06	3.18	7.63
			av 4.06 ± 0.07		av 8.02 ± 0.16

[a] Reference 6.

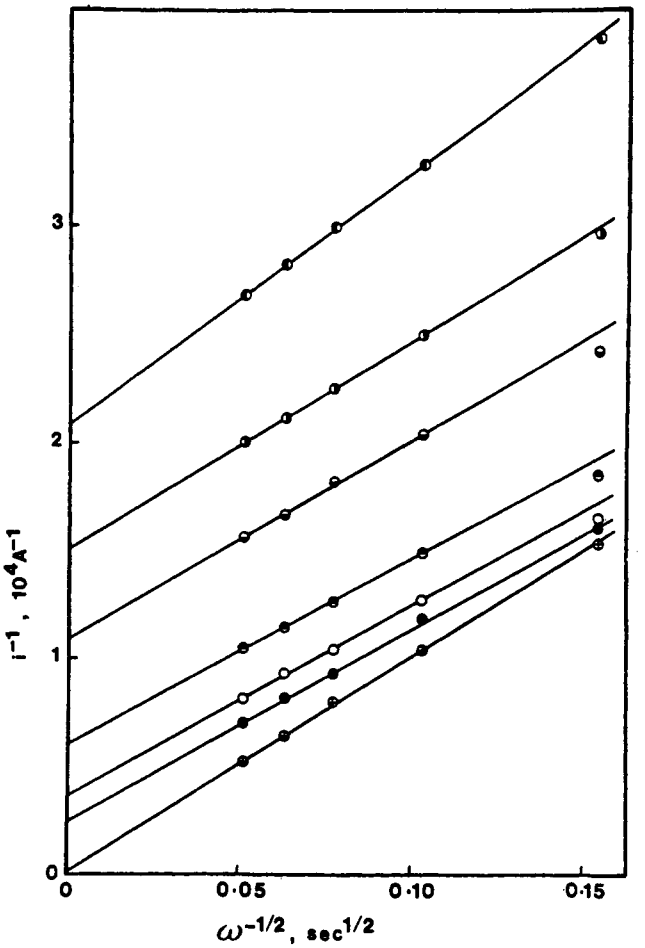

Figure 12. Plots of i^{-1} vs. $\omega^{-1/2}$ for 20.4×10^{-3} M Sb(IIIe in 0.75:1 melt. Potentials from top to bottom: 0.38, 0.39, 0.40, 0.42, 0.44, 0.46, 0.60 V.

of i_{lc}, at potentials on the limiting plateau, vs. $\omega^{1/2}$ was linear (Figure 7b), indicating that the reduction of Sb(V) to Sb(III) is diffusion controlled on the plateau. Thus, from the Levich equation (eq 3) and i_{la} and i_{lc} for Sb(III) and Sb(V), the diffusion coefficients for Sb(III) and Sb(V) can be calculated, and the results of these calculations are tabulated in Table III. The ηD products, also tabulated in Table III, were found to be quite constant across the entire basic region for both Sb(III) and Sb(V) species. Thus, the Stokes–Einstein relation was obeyed. Values calculated from eq 4 give 5.56 Å for the Sb(III) and 2.86 Å for the Sb(V) species. A smaller ionic radius for the Sb(V) species than for the Sb(III) species is expected in view of the smaller ionic radius of Sb(V). This large difference between the ionic radii, however, may indicate Sb(III) to be more solvated than the Sb(V) species, perhaps

Table IV. Dependence of α and $k^{\ominus}$ for the Sb(III)/Sb(V) System on Melt Composition

N_A/N_B	α	$k^{\ominus}$, 10^{-4} cm s^{-1}
0.75	0.26[a]	1.4[a]
0.75	0.50[b]	1.8[c]
0.80	0.50[b]	3.4[c]
0.91	0.50[b]	3.8[c]

[a] From rotating disk experiment. [b] Assumed value. [c] From cyclic voltammetry.

by $AlCl_4^-$. Comments above regarding the applicability of a modified form the Stokes–Einstein equation are still valid.

As shown in Figure 12, plots of i^{-1}, at various potentials on the rising portion of the RGCDE waves in Figure 6, vs. $\omega^{-1/2}$ were linear with an intercept indicating a charge-transfer rate determining process. These plots were used to evaluate the rate constant according to

$$1/i = 1/i_k + 1/0.620nFAC^*D^{2/3}\nu^{-1/6}\omega^{1/2} \quad (12)$$

where

$$i_k = nFAk_fC^* \quad (13)$$

and k_f is the charge-transfer rate constant at a given potential. A plot of ln k_f vs. E (Figure 13) is linear, as expected from the relation for an anodic process

$$k_f = k^{\ominus} \exp[-(1-\alpha)n_aF(E - E^{\circ\prime})/RT] \quad (14)$$

where $k^{\ominus}$ is the rate constant at a formal potential $E^{\circ\prime}$, α is the transfer coefficient, and n_a is the number of electrons involved in the rate-determining step. Values of $k^{\ominus}$ at $E^{\circ\prime}$ obtained from eq 10 for $n_a = 1$ are given in Table IV.

Analyses of cyclic voltammograms, for the anodic wave and its corresponding cathodic wave in the reverse scan for three different basic melt Sb(III) solutions, are given in Table V. The shift in the peak potentials with scan rate also indicated a kinetically controlled electron-transfer process. A plot of

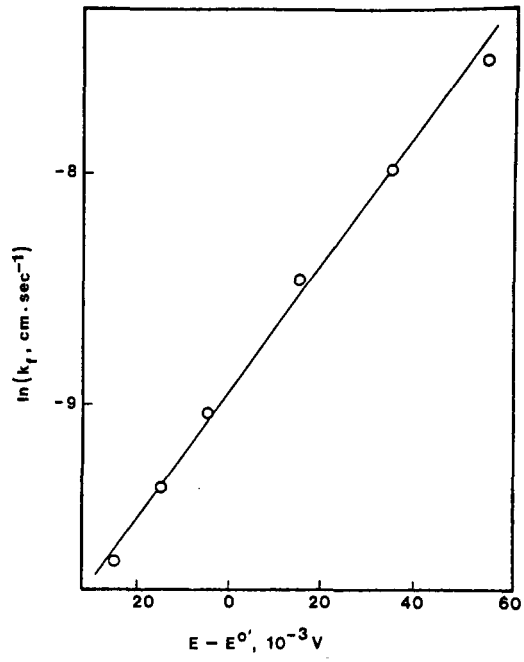

Figure 13. Plot of ln k_f vs. $(E - E^{\circ\prime})$ for 20.4×10^{-3} M Sb(III) in 0.75:1 melt.

$E_{p_a} - E_{p/2}$ vs. $v^{1/2}$ was linear, indicating a quasi-reversible behavior. At low scan rates the value for $E_{p_a} - E_{p/2}$ approaches that for a reversible process. Thus, $E_{1/2}$ was estimated for these scans from the relation

$$E_{p/2} = E_{1/2} + 1.109RT/2F \quad (15)$$

and the results are shown in Table V. These values of $E_{1/2}$ were used to calculate $E^{\circ\prime}$, from the relation

$$E^{\circ\prime} = E_{1/2} + (RT/2F) \ln [D_{Sb(V)}/D_{Sb(III)}]^{1/2} \quad (16)$$

Values of $E^{\circ\prime}$ obtained in this way were in good agreement

Table V. Dependence of E_{p_a}, E_{p_c}, ΔE_p, $E_{p/2}$, $E_{p_a} - E_{p/2}$, $E_{1/2}$, and $E^{\circ\prime}$ for Sb(V)/Sb(III) on the Melt Composition

N_A/N_B	v, mV s^{-1}	E_{p_a}, V	E_{p_c}, V	ΔE_p, mV	$E_{p/2}$, V	$E_{p_a} - E_{p/2}$, mV	$E_{1/2}$, V	$E^{\circ\prime}$,[a] V	$E^{\circ\prime}$,[b] V	$E^{\circ\prime}_2$,[c] V
0.75	5	0.425	0.370	55	0.385	40	0.400	0.405	0.407	0.410
	10	0.425	0.365	60	0.385	40	0.400	0.405		
	20	0.435	0.365	70	0.390	45				
	50	0.450	0.350	100	0.400	50				
	100	0.455	0.340	115	0.400	55				
	200	0.480	0.330	150	0.415	65				
0.79									0.412	0.410
0.80	5	0.430	0.390	40	0.395	35	0.410	0.415	0.414	0.410
	10	0.430	0.380	50	0.395	35	0.410	0.415		
	20	0.435	0.370	65	0.400	40				
	50	0.445	0.370	75	0.400	45				
	100	0.455	0.360	95	0.405	50				
	200	0.470	0.350	120	0.410	60				
	500	0.490	0.335	155	0.415	75				
0.82									0.417	0.411
0.83									0.420	0.412
0.87									0.427	0.411
0.91	5	0.445	0.400	45	0.415	30	0.430	0.435	0.437	0.411
	10	0.450	0.400	50	0.415	35	0.430	0.435		
	20	0.455	0.395	60	0.415	40				
	50	0.465	0.385	80	0.420	45				
	100	0.475	0.380	95	0.425	50				
	200	0.485	0.365	120	0.425	60				
	500	0.510	0.350	160	0.435	75				
0.92									0.439	0.410
0.93									0.442	0.409
0.97									0.462	0.406

[a] $E^{\circ\prime} = E_{1/2} + (RT/2F) \ln (D_{Sb(V)}/D_{Sb(III)})^{1/2}$. [b] $E^{\circ\prime} = E_{eq} - (RT/2F) \ln ([Sb(V)]/[Sb(III)])$. [c] $E^{\circ\prime}_2 = E_{eq} - (RT/2F) \ln ([Sb(V)]/[Sb(III)]) + ((p_2 - p_1)RT/2F) \ln [Cl^-]$.

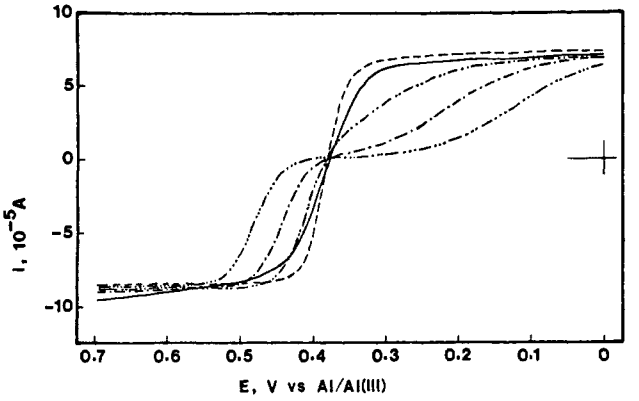

Figure 14. Comparison between an experimental RGCDE voltammogram (solid line), obtained for a solution of 13.7×10^{-3} M Sb(III) and 6.7×10^{-3} M Sb(V) in 0.75:1 melt with a rotation rate of 1600 rpm, and those calculated by using assumed parameters for and *EEC* mechanism ($\alpha_1 = 0.5$): ---, $E^{\ominus}_{s,1} = E^{\ominus}_{s,2} = 0.407$ V, $k^{\ominus}_{s,1} = 10^{-3}$ cm s^{-1}; ---, $E^{\ominus}_{s,1} = E^{\ominus}_{s,2} = 0.407$ V, $k^{\ominus}_{s,1} = 10^{-5}$ cm s^{-1}; ····, $E^{\ominus}_{s,1} = 0.500$ V, $E^{\ominus}_{s,2} = 0.314$ V, $k^{\ominus}_{s,1} = 10^{-5}$ cm s^{-1}; ·····, $E^{\ominus}_{s,1} = 0.300$ V, $E^{\ominus}_{s,2} = 0.514$ V, $k^{\ominus}_{s,1} = 10^{-5}$ cm s^{-1}.

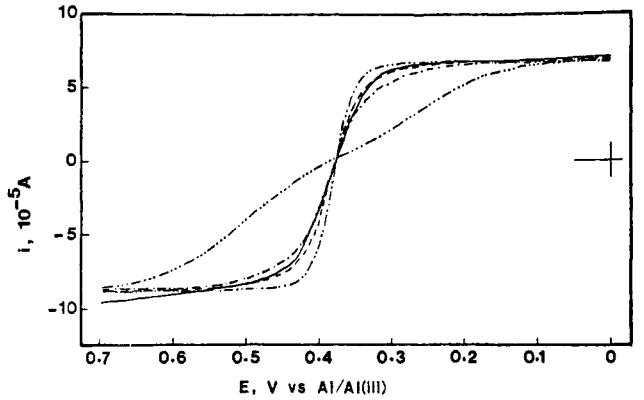

Figure 15. Comparison between an experimental RGCDE voltammogram (solid line), obtained for a solution of 13.7×10^{-3} M Sb(III) and 6.7×10^{-3} M Sb(V) in 0.75:1 melt with a rotation rate of 1600 rpm, and those calculated by using assumed sets of parameters for an *EEC* mechanism ($\alpha_1 = \alpha_2 = 0.5$, $E^{\ominus}_{s,1} = 0.200$ V, $E^{\ominus}_{s,2} = 0.614$ V). $k^{\ominus}_{s,1} = k^{\ominus}_{s,2}$ (cm s^{-1}): ····, 0.1; ---, 0.02, ---, 0.01; ·····, 0.001.

with those obtained from potentiometric measurements (Table V).

The peak separations $E_{p_a} - E_{p_c}$, reported in Table V, were used to estimate $k^{\ominus}$ by using a method reported by Nicholson.[35] According to this method, a parameter ψ, defined by

$$\psi = (D_R/D_O)^{(1-\alpha)/2} k^{\ominus} [D_R \pi v (nF/RT)]^{1/2} \quad (17)$$

was estimated from the variation of $E_{p_a} - E_{p_c}$ with scan rate. Data for $k^{\ominus}$, obtained in this way assuming $\alpha = 0.5$, are reported in Table IV and are in reasonable agreement with that obtained from the RGCDE voltammograms.

An attempt was made to draw conclusions on the mechanism of the electrode process, and models 1 and 2 were suggested. The symmetry of the voltammograms at the RGCDE

model 1 (*EEC* mechanism)

$$SbCl_6^- + e^- \xrightarrow{\text{slow}} SbCl_6^{2-} \quad E^{\ominus}_{s,1},\ k^{\ominus}_{s,1},\ \alpha_1$$

$$SbCl_6^{2-} + e^- \xrightarrow{\text{fast}} SbCl_6^{3-} \quad E^{\ominus}_{s,2}$$

$$SbCl_6^{3-} \xrightarrow{\text{fast}} SbCl_4^- + 2Cl^-$$

$$\text{net: } SbCl_6^- + 2e^- \rightarrow SbCl_4^- + 2Cl^-$$

model 2 (*EEC* mechanism)

$$SbCl_6^- + e^- \xrightarrow{\text{slow}} SbCl_6^{2-} \quad E^{\ominus}_{s,1},\ k^{\ominus}_{s,1},\ \alpha_1$$

$$SbCl_6^{2-} + e^- \xrightarrow{\text{slow}} SbCl_6^{3-} \quad E^{\ominus}_{s,2},\ k^{\ominus}_{s,2},\ \alpha_2$$

$$SbCl_6^{3-} \rightarrow SbCl_4^- + 2Cl^-$$

$$\text{net: } SbCl_6^- + 2e^- \rightarrow SbCl_4^- + 2Cl^-$$

(Figure 11) supports a slow double one-electron-transfer process (model 2); nevertheless, both models were considered. Steady-state waves calculated from various sets of parameters for both models are shown and compared with an experimental voltammogram in Figures 14 and 15. These calculations gave support for model 2 and, as expected, calculated waves for model 1 were asymmetrical, unlike the experimental wave; the only symmetrical wave based on model 1 (Figure 14) was much steeper than the experimental one, and certainly the value of the rate constant used to calculate this wave was 1 order of magnitude higher than the values reported in Table IV.

Acknowledgment. The aid of Dr. Tadeusz Hepel in performing the calculations on the mechanism of the electrode reaction is gratefully acknowledged. This work was supported by the Air Force Office of Scientific Research.

Registry No. $SbCl_2^+$, 73740-59-7; $SbCl_4^-$, 18443-80-6; $SbCl_6^-$, 17949-89-2; $AlCl_3$, 7446-70-0; $SbCl_3$, 10025-91-9; Sb, 7440-36-0; C, 7440-44-0; BuPyCl, 1124-64-7.

(35) Nicholson, R. S. *Anal. Chem.* **1965**, *37*, 1351.